Annual progress report – November 2007

# Thermomechanical Fatigue Characterization of 60-NiTi SMAs


**Texas A&M University**

Dr. Dimitris C. Lagoudas
Olivier W. Bertacchini
Justin Schick

**The Boeing Company**

Dr. Frederick T. Calkins
James J. Mabe

Contents

# 1. Introduction

## 1.1. Motivations and objectives

With the purpose of developing new actuation technologies incorporating active materials, including designing systems which provide significant noise reduction of commercial aircraft, Boeing engineers have been studying a new composition for a NiTi shape memory alloy: 60-NiTi. In previous research efforts, development, characterization and modeling of the material were the main objectives with little effort dedicated to the understanding of the material's fatigue behavior. As the technology continues to mature, such an understanding has now become pertinent. One illustration of the need for fatigue characterization of SMAs is the Boeing Variable Geometry Chevron (VGC). This component is subject to one cycle per flight. Current airliners undergo approximately 20K to 70K flight cycles, therefore the designed VGC can be expected to undergo 20K to 70K cycles during its service life. In order to be integrated in an aerospace structure in the near future, the SMA materials must demonstrate sufficient fatigue life such that they can complete their service life while also considering some safety margin.

The primary goal is to collect fatigue data which will help ascertain the capacity of the 60-NiTi to serve as an actuating material. In addition, the failure mechanisms are to be studied to relate process, microstructure and fatigue properties through fractography. Finally, the influence of parameters such as the specimen thickness and the type of heat treatment is to be scrutinized for optimization purpose.

## 1.2. Proposed methodology

To test the ability of 60-NiTi to demonstrate the capacity to sustain a sufficient amount of thermomechanical fatigue cycles plus some safety margin, 60-NiTi samples were prepared by Boeing engineers as flat dogbone specimens and used to perform isobaric thermal cycles. The fatigue experimental setup in the Active Materials Laboratory at Texas A&M University allows testing of very small specimens. Therefore, three different narrow cross sections were selected to determine what effects, if any, the size and geometric configuration of the specimens have on their fatigue life. A stress range was selected, which included the working stresses of proposed applications plus some margin of safety. Two different heat treatments were selected, with an additional parameter being the heat treatment environment (vacuum and air).

## 2. Experimental setup

### 2.1. Material system and specimens' geometry

The material used in this work is a Ni-rich NiTi Shape Memory Alloy 60Ni40Ti (wt.%). The geometry of the specimens was driven by the actual VGC geometry. Therefore thin dogbones with a thickness to width ratio similar to the one seen in the actual SMA actuators mounted onto the VGCs.

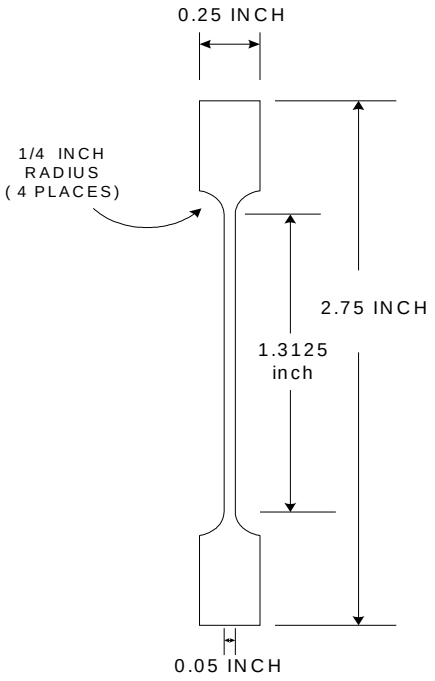


While the length of the specimen is defined as shown above, three different thicknesses were selected to assess any size effect on the fatigue life. The three selected thicknesses were 0.005, 0.010 and 0.015 inches.

### 2.2. Heat treatments and transformation temperatures for 60-NiTi

One particular property of the Ni-rich 60-NiTi SMA is that it can exhibit SME without any cold work process. The presence of precipitates favors the storing of elastic energy and therefore the realization of recoverable strains upon martensitic phase transformation. The proportions, the distribution and the composition of the precipitates can be modified / adjusted by applying appropriate heat treatments. The heat treatments consist of a homogenization treatment of one hour at 850°C with furnace controlled cooling to allow formation of precipitates followed by an annealing treatment of either 1 or 20 hours at 450°C.

After the selection of two different heat treatments, HT#1 and HT#2, the determination of the transformation temperatures is needed to characterize any differences due to microstructural modifications in terms of precipitates. For this purpose,

a differential scanning calorimeter (DSC) was used to determine the transformation temperatures under zero-stress. The method of intersecting tangents was used to determine the zero-stress transformation temperatures indicated in the table below.

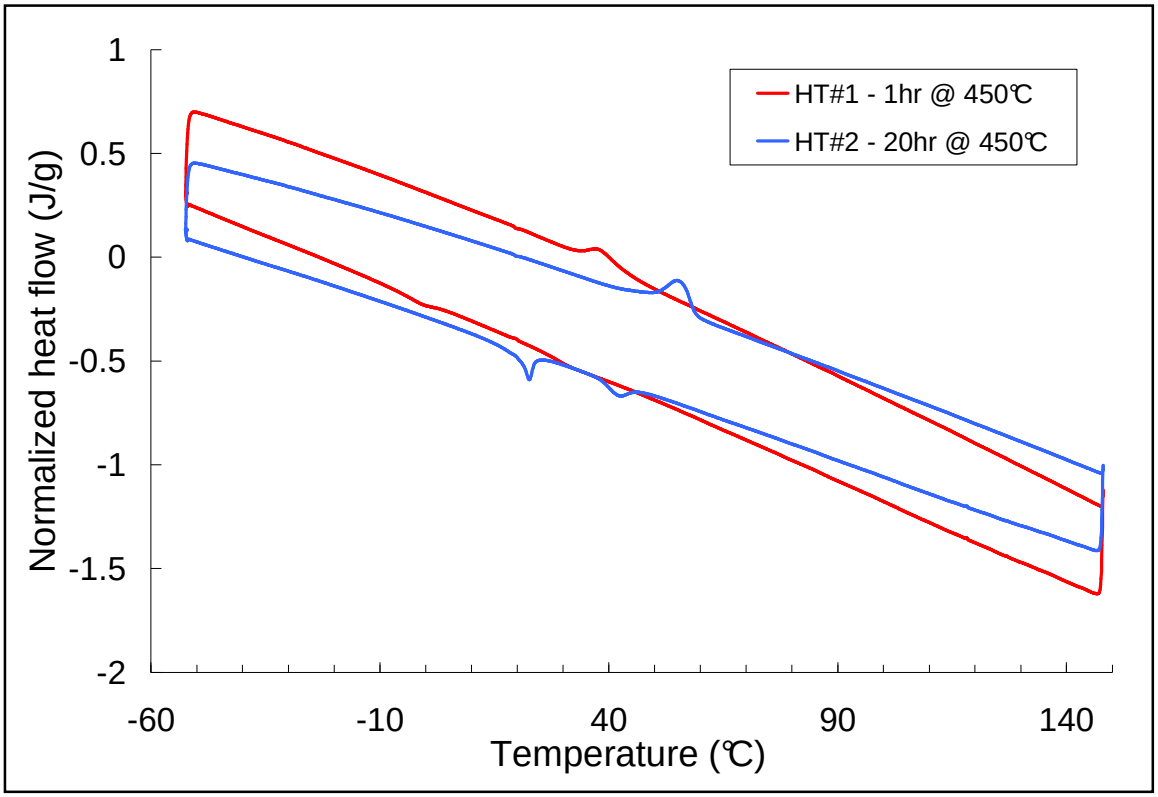


| | | | |
|---|---|---|---|
| HT#1 | $M^{os}$ = 3.5°C<br>$M^{of}$ = -8.5°C | $R^{os}$ = 42.5°C<br>$R^{of}$ = 25.0°C | $A^{os}$=32.5°C<br>$A^{of}$=45.5°C |
| HT#2 | $M^{os}$ = 24.0°C<br>$M^{of}$ = 17.5°C | $R^{os}$ = 46.5°C<br>$R^{of}$ = 37.5°C | $A^{os}$=40.0°C<br>$A^{of}$=59.0°C |

The results indicate a significant increase of the transformation temperatures of HT#2.

### 2.3.Thermomechanical fatigue testing apparatus

The identification of the loading conditions of the SMA components led to the definition of a series of uniaxial isobaric thermally induced fatigue tests. The following schematic represents the stress-temperature phase diagram of NiTi SMAs. The red horizontal double arrow indicates the isobaric loading path and the selected stress levels are 50 MPa, 150 MPa and 250 MPa. The maximum working stress identified in the SMA beam in full actuation with the VGC was determined using finite element calculation and gave a value of ~100MPa. Therefore by testing up to 250 MPa, one can account for safety margin and overload conditions.

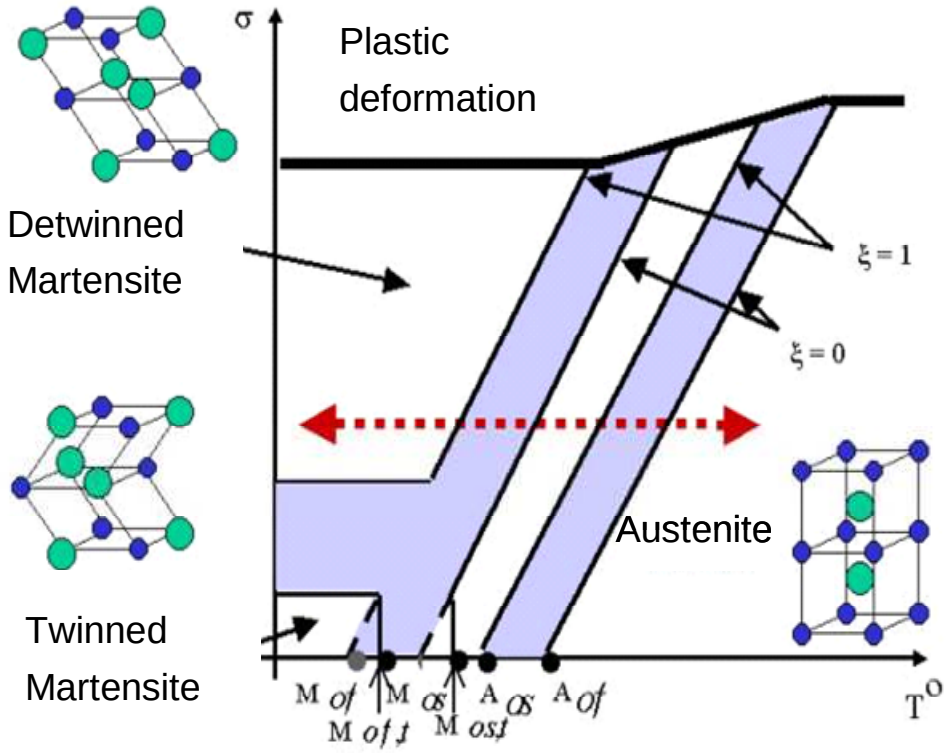


The following schematic and picture are a side-view and top-view of the custom built fatigue frame used at Texas A&M University. It consists of a Plexiglas bath containing a closed-loop circulating coolant allowing to achieve forced fluid convective cooling onto specimens immerged in the bath. The coolant is a waterless solution of ethylene and propylene glycol. Heating is achieved through resistive Joule heating using a DC power supply connected to the two ends of the specimens. The specimens are mounted from one end to a fixed point on a rigid aluminum frame while the other end is connected to masses hanging vertically through a pulley system. Displacement measurement is achieved using linear variable displacement transducers (LVDTs) connected from the rigid frame to the free-end of the specimens connected to the hanging weight. The displacements of the SMA actuators are recorded through LVDT transducers and the strains in the austenitic and martensitic states are used to define total, plastic and recoverable strains.

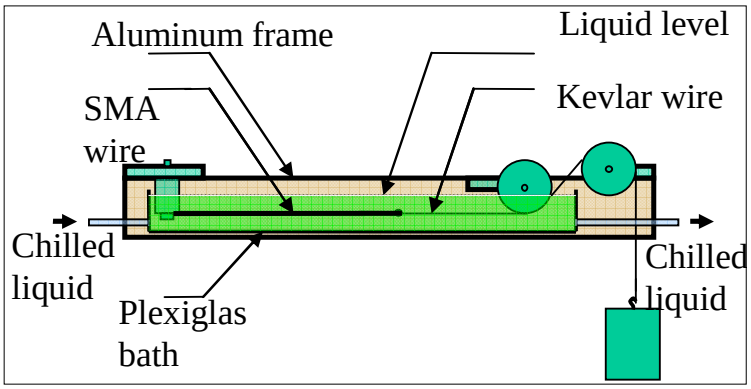

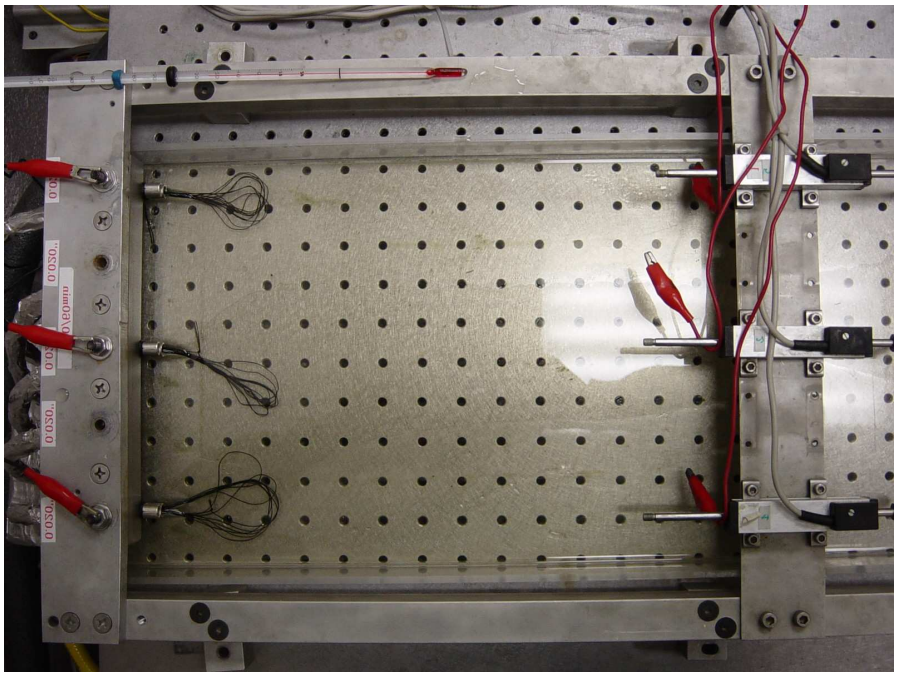

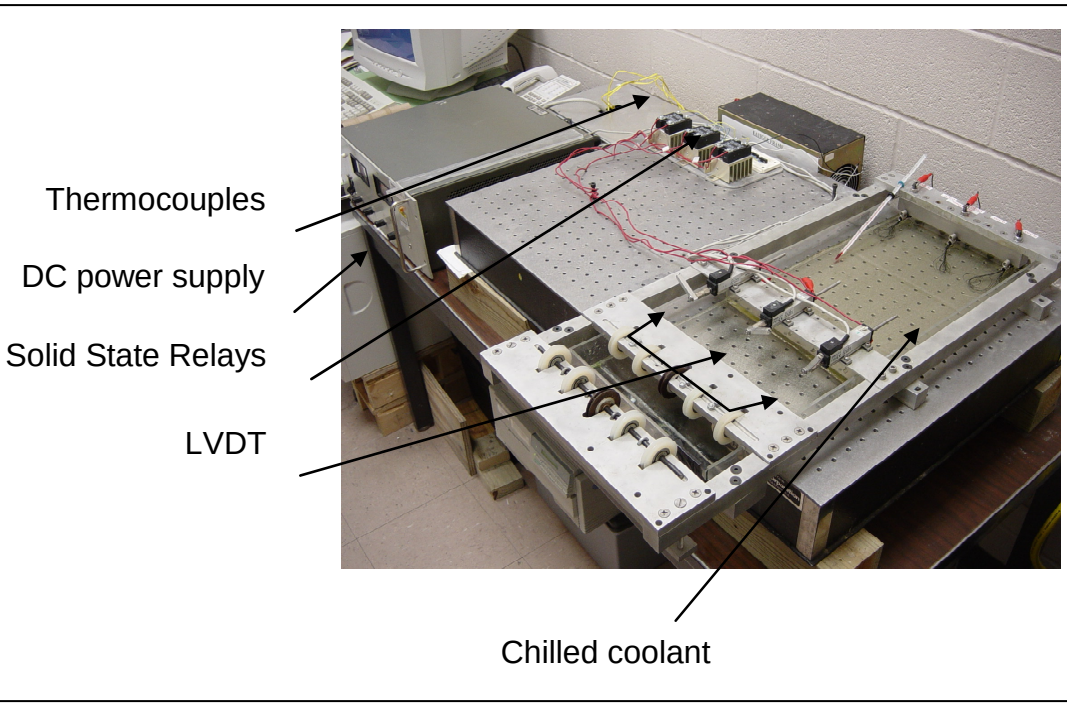


Thermal loading cycles are achieved at a frequency close to 0.2 Hz. The advantage of such design is the capacity to produce thermomechanical fatigue data between 48 hours and one week in average.

The relatively high cycling frequency may have some influence on the completion of the thermomechanical transformation cycles undergone in the SMA specimens. Therefore, near quasi-static thermal actuation tests were achieved on a MTS loading stage. The

following schematics indicate the loading path applied for each constant applied stress level and is represented for the two different heat treatments, HT#1 and HT#2, in terms of the zero-stress transformation temperatures.

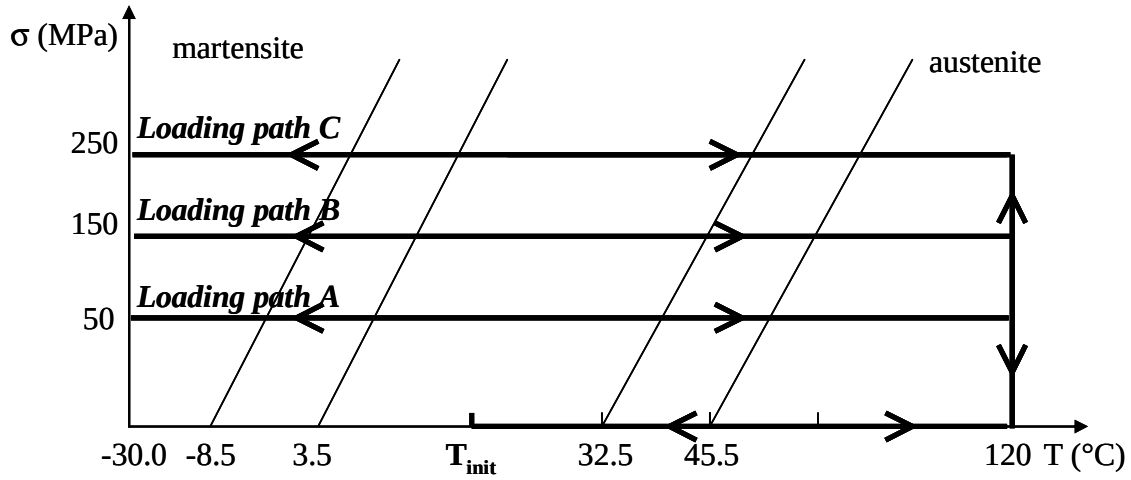


Heat treatment #1, $T_{init}$ = room temperature.

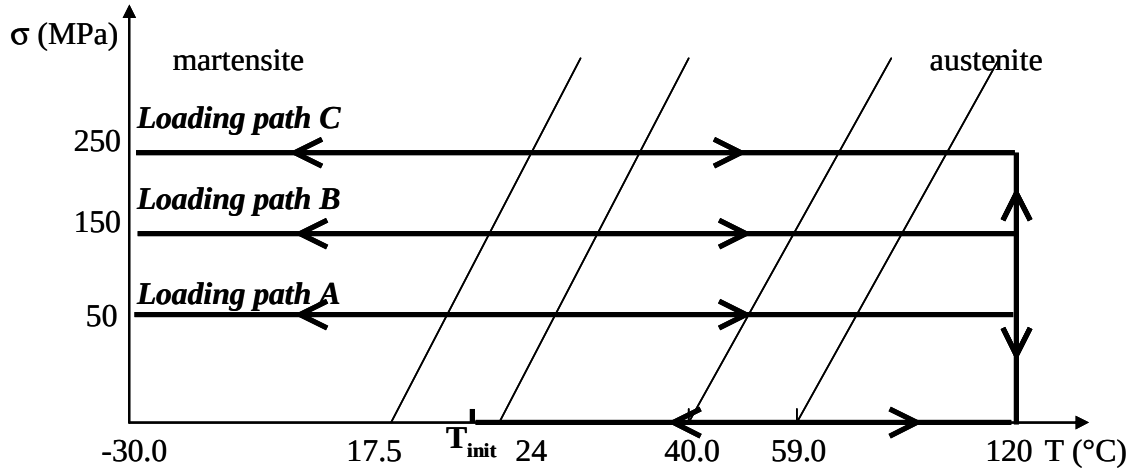


Heat treatment #2, $T_{init}$ = room temperature.

The results are shown in the following strain-temperature curves.

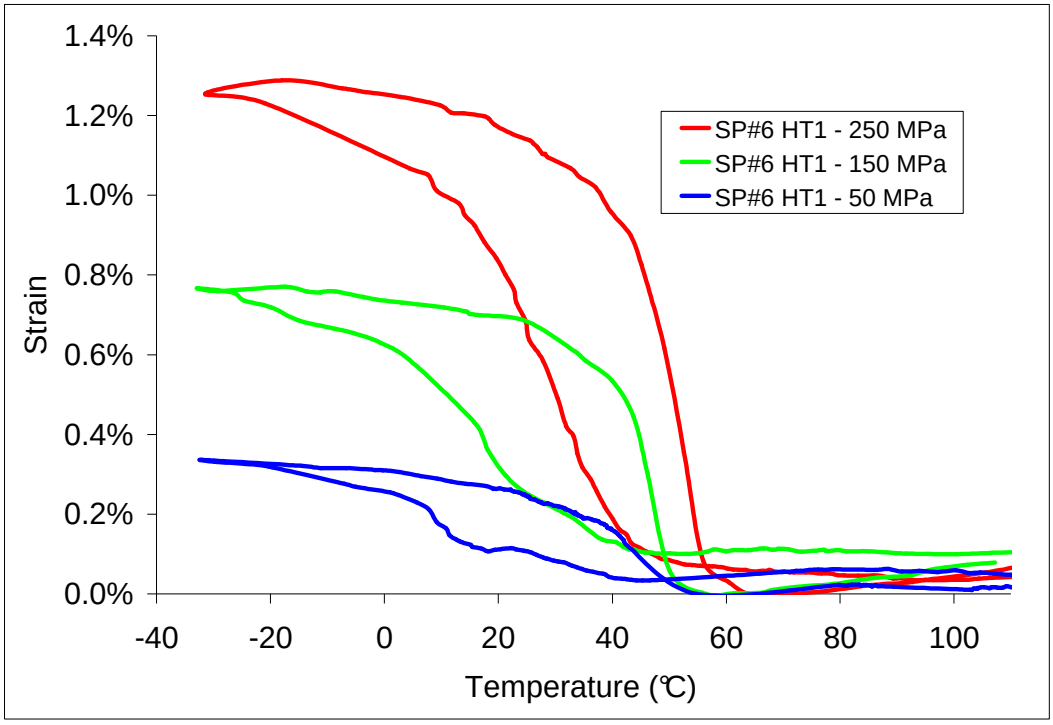
1.4%
1.2%
1.0%
0.8%
0.6%
0.4%
0.2%
0.0%
Strain
-40
-20
0
20
40
60
80
100
Temperature (℃)
SP#6 HT1 - 250 MPa
SP#6 HT1 - 150 MPa
SP#6 HT1 - 50 MPa

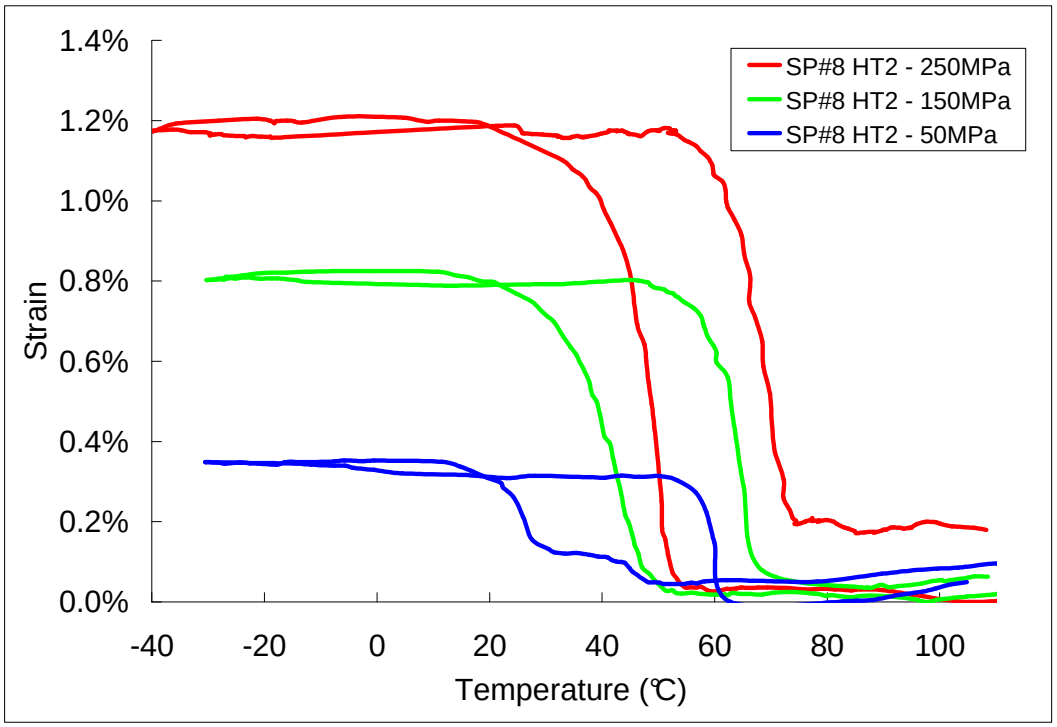
1.4%
1.2%
1.0%
0.8%
0.6%
0.4%
0.2%
0.0%
Strain
-40
-20
0
20
40
60
80
100
Temperature (℃)
SP#8 HT2 - 250MPa
SP#8 HT2 - 150MPa
SP#8 HT2 - 50MPa

The amount of recoverable strain generated for both HT#1 and HT#2 from the quasi-static testing are reported in the following table and are compared to values obtained in the fatigue frame.

| | 50MPa (HT#1 / HT#2) | 150MPa (HT#1 / HT#2) | 250MPa (HT#1 / HT#2) |
|---|---|---|---|
| MTS loading stage | 0.35% / 0.35% | 0.7% / 0.75% | 1.3% / 1.0% |
| Fatigue frame | X / 0.35% | 0.6% / 0.7% | 1.1% / 1.0% |

In addition to the validation that the fatigue frame can perform as well as the MTS loading stage in terms of amount of recoverable strain, another feature from the different heat treatments has been identified. The amount of latent heat of transformation in the case of HT#1 was smaller than in the case of HT#2. The specimen exhibiting the least amount of latent heat of transformation (HT#1) was characterized by a more gradual transformation occurring upon thermal loading under the application of constant stress while the specimen exhibiting the highest amount of latent heat of transformation displayed a sharp and quick transformation under the same conditions. This is another indication that microstructural differences were generated with the application of two different heat treatments.

## 3. Ni60Ti40 fatigue results

### 3.1. Representative fatigue data

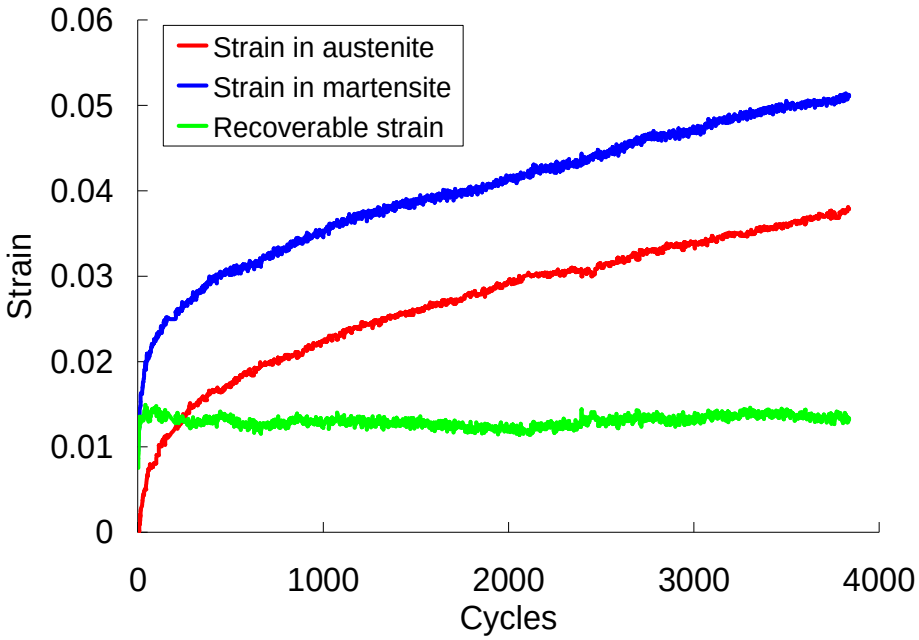


HT1, 250 MPa, thickness = 10 mils

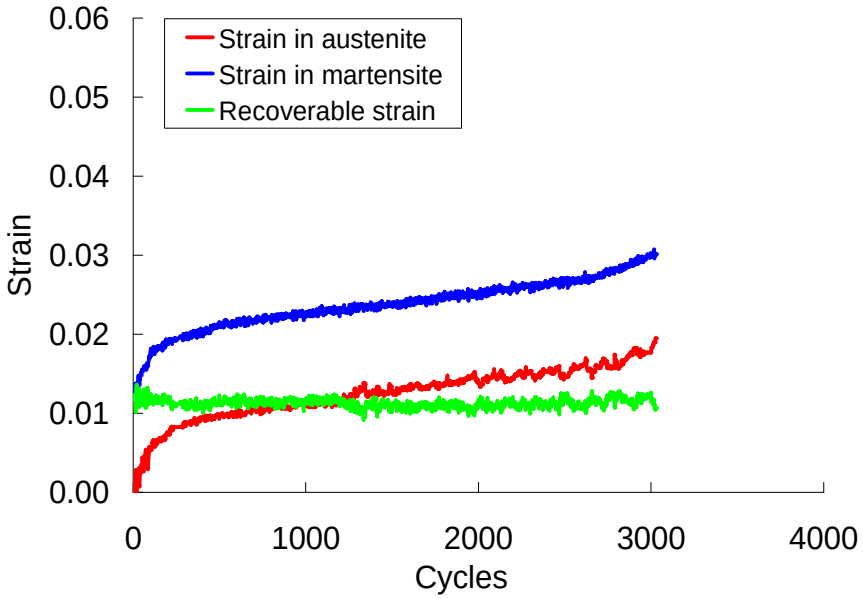


HT2, 250 MPa, thickness = 5 mils

### 3.2. Recoverable strain – Applied stress level

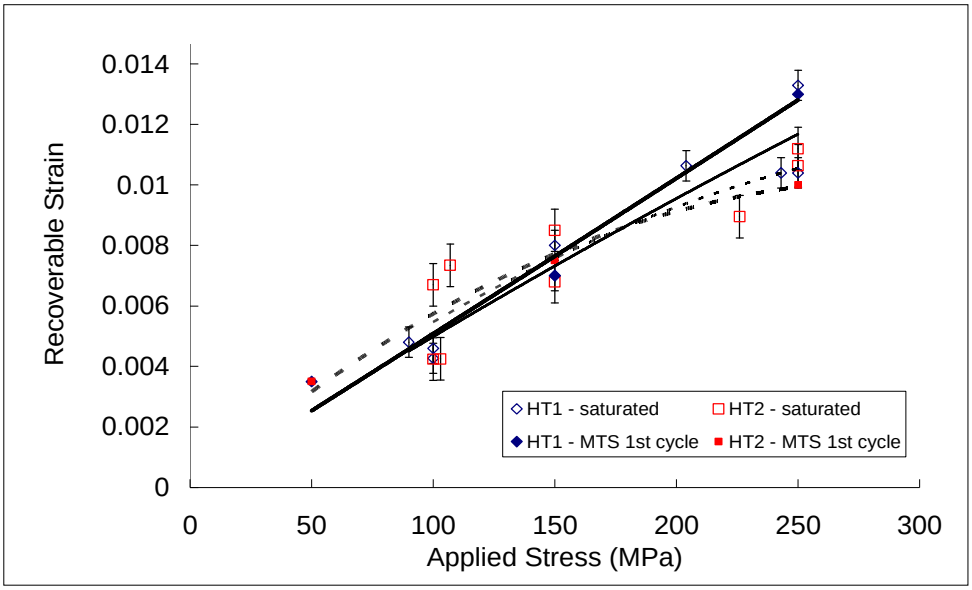


Calibration on MTS (1st cycle - thick trend lines) compared to values recorded at saturation (thin trend lines). Similar trend observed between initial and saturated recoverable strain in both heat treatments

### 3.3. Applied Stress – Life

Very little influence from the different heat treatments on fatigue life for a given applied stress level. No significant size effect on the service life of the SMA actuators

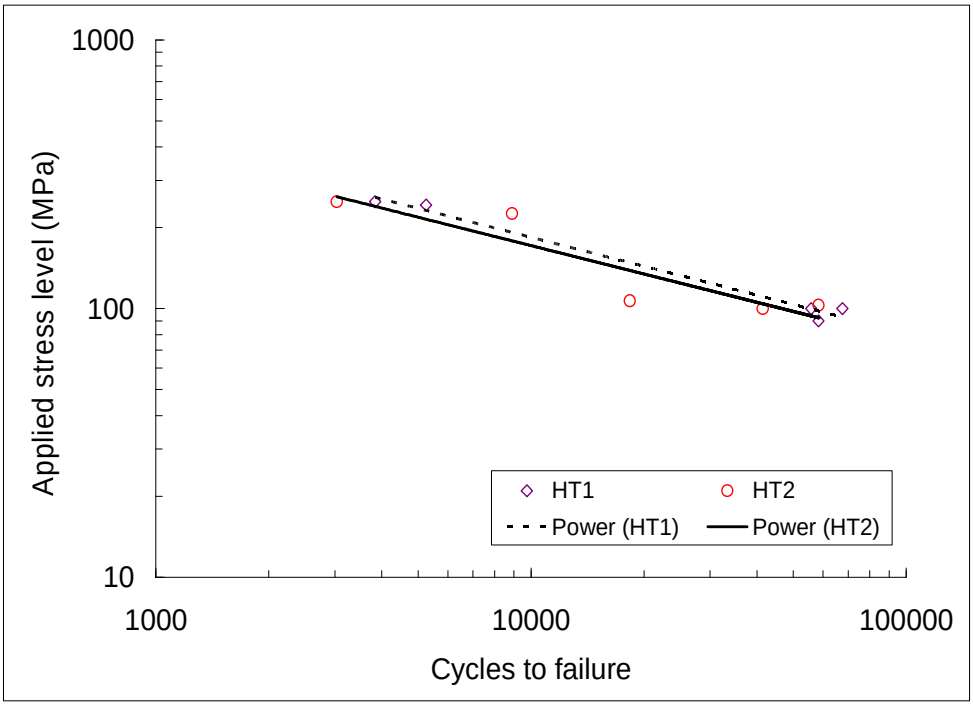

### 3.4. Plastic strain – Life

Accumulated plastic strain values calculated from the non-recovered strain in austenite.

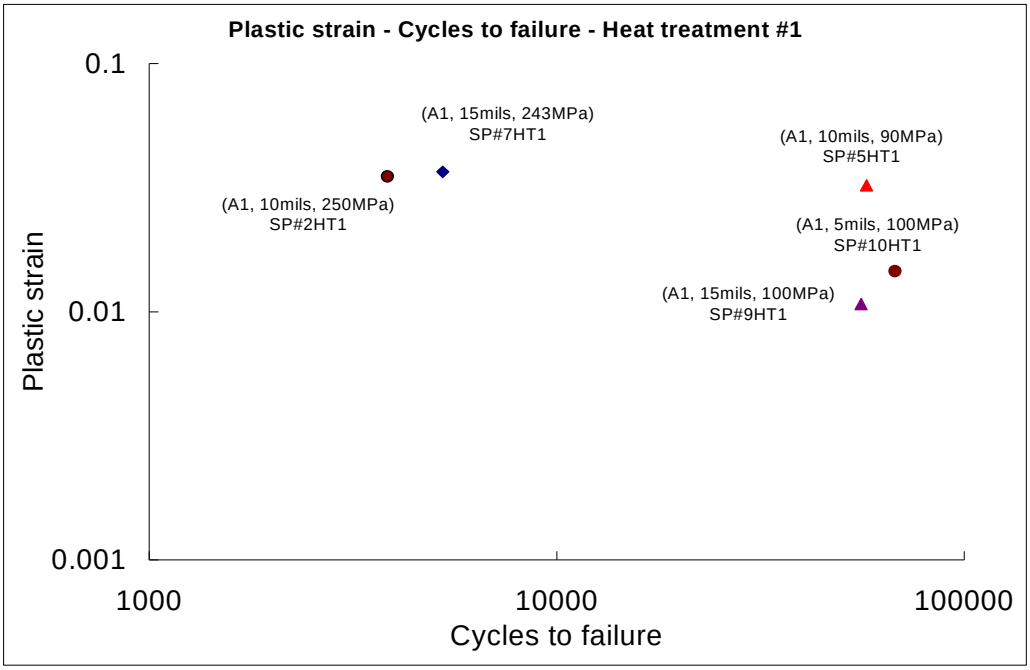


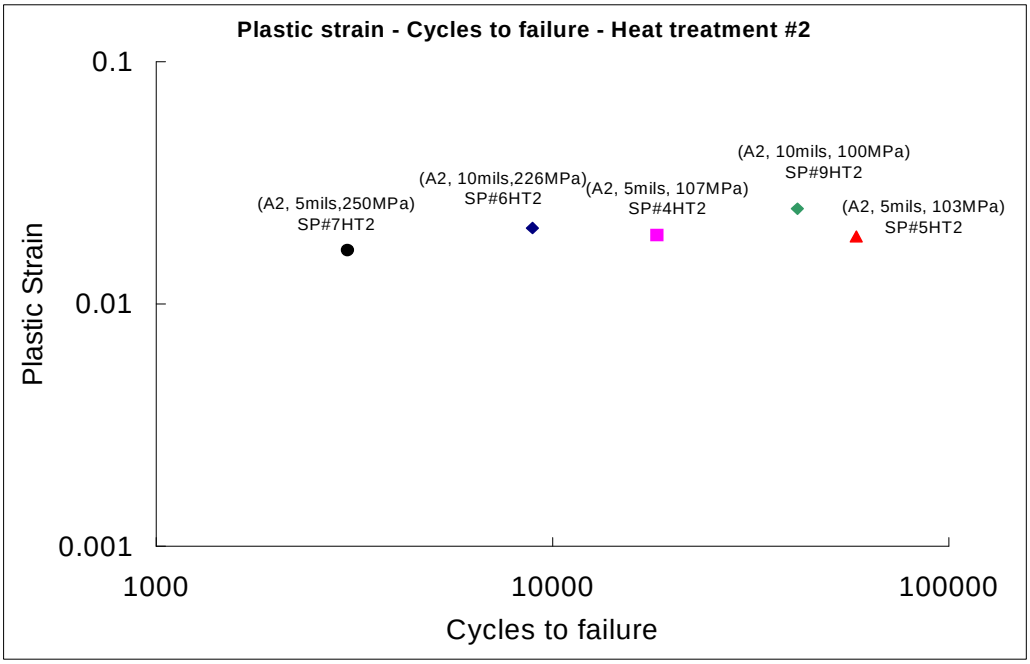


Amount of plastic strain represents the amount of damage/defects accumulated throughout the cycles

**⇒ Possibility to define a failure criterion through saturated plastic at failure.**

A summary of the test specimens, the testing conditions and the testing order is given in the following table.
Tables identifying the run orders and the loading conditions applied to each run.

| Run order | Specimen # | Heat treatment | Thickness (mils) | Applied stress (MPa) |
|---|---|---|---|---|
| *1* | *SP# 6 HT2* | *A2* | *10* | *226* |
| *2* | *SP# 4 HT2* | *A2* | *5* | *107* |
| *3* | *SP# 3 HT1* | *A1* | *5* | *204* |
| *4* | *SP# 7 HT1* | *A1* | *15* | *243* |
| *5* | *SP# 5 HT2* | *A2* | *5* | *103* |
| *6* | *SP# 5 HT1* | *A1* | *10* | *90* |
| *7* | *SP# 3 HT2* | *A2* | *15* | *142* |
| *8* | *SP# 7 HT2* | *A2* | *5* | *250* |
| *9* | *SP# 2 HT1* | *A1* | *10* | *250* |
| *10* | *SP# 4 HT1* | *A1* | *15* | *203* |
| *11* | *SP# 8 HT1* | *A1* | *10* | *100* |
| *12* | *SP# 9 HT1* | *A1* | *15* | *100* |
| *13* | *SP# 10 HT1* | *A1* | *5* | *100* |
| *14* | *SP# 9 HT2* | *A2* | *10* | *100* |
| *15* | *SP# 10 HT2* | *A2* | *10* | *250* |
| Heat Treatments | | A1 | 1 hr @ 850℃, 1 hr @ 450℃ | |
| | | A2 | 1 hr @ 850℃, 20 hrs @ 450℃ | |

Table summarizing erroneous tests with invalid results.

| | |
|---|---|
| SP# 1 HT1 | Damaged during preliminary testing |
| SP# 1 HT2 | Damaged during preliminary testing |
| SP# 2 HT2 | Not applicable for isobaric uniaxial fatigue testing<br>irregular cross section with major notches |
| SP# 6 HT1 | MTS tested |
| SP# 8 HT2 | MTS tested |
| SP# 5 HT1 | No failure (run out at ~60K cycles) |
| SP# 5 HT2 | No failure (run out at ~60K cycles) |
| SP# 4 HT1 | Invalid results (computer malfunction) |

The last table is a collection of the fatigue results in terms of recoverable strain and accumulated plastic strain at half the life and at failure life of the tested specimens.

Comprehensive results for water jet processed specimens for heat treatment #1.

The following table is ordered according to increasing sample thickness

| HT1 - 1 hr @ 850℃, 1 hr @ 450℃ | | | | | | | |
|---|---|---|---|---|---|---|---|
| Specimen number | Thickness (mils) | Applied stress (MPa) | Cycles to failure Nf | Recoverable strain @ 1/2 Nf | Plastic strain @ 1/2 Nf | Recoverable strain @ Nf | Plastic strain @ Nf |
| 3 | 5 | 204 | 6896 | 0.01073 | 0.00257 | 0.01063 | 0.00685 |
| 10 | 5 | 100 | 67571 | 0.00464 | 0.00861 | 0.0046 | 0.01457 |
| 2 | 10 | 250 | 3838 | 0.01209 | 0.02585 | 0.01329 | 0.03511 |
| 5 | 10 | 90 | 57598 (run out) | 0.00583 | 0.01337 | 0.0048 | 0.0323 |
| 7 | 15 | 243 | 5251 | 0.0106 | 0.026 | 0.0104 | 0.03667 |
| 9 | 15 | 100 | 55811 | 0.00383 | 0.00726 | 0.00427 | 0.01074 |
| 1 | *Damaged during preliminary testing* | | | | | | |
| 4 | *Invalid results (computer malfunction)* | | | | | | |
| 6 | *MTS tested* | | | | | | |
| 8 | *Invalid results (computer malfunction)* | | | | | | |

The following table is ordered according to increasing applied stress level.

| HT1 - 1 hr @ 850℃, 1 hr @ 450℃ | | | | | | | |
|---|---|---|---|---|---|---|---|
| Specimen number | Thickness (mils) | Applied stress (MPa) | Cycles to failure Nf | Recoverable strain @ 1/2 Nf | Plastic strain @ 1/2 Nf | Recoverable strain @ Nf | Plastic strain @ Nf |
| 5 | 10 | 90 | 57598 (run out) | 0.00583 | 0.01337 | 0.0048 | 0.0323 |
| 9 | 15 | 100 | 55811 | 0.00383 | 0.00726 | 0.00427 | 0.01074 |
| 10 | 5 | 100 | 67571 | 0.00464 | 0.00861 | 0.0046 | 0.01457 |
| 3 | 5 | 204 | 6896 | 0.01073 | 0.00257 | 0.01063 | 0.00685 |
| 7 | 15 | 243 | 5251 | 0.0106 | 0.026 | 0.0104 | 0.03667 |
| 2 | 10 | 250 | 3838 | 0.01209 | 0.02585 | 0.01329 | 0.03511 |
| 1 | *Damaged during preliminary testing* | | | | | | |
| 4 | *Invalid results (computer malfunction)* | | | | | | |
| 6 | *MTS tested* | | | | | | |
| 8 | *Invalid results (computer malfunction)* | | | | | | |

Comprehensive results for water jet processed specimens for heat treatment #2.

The following table is ordered according to increasing sample thickness.

| HT2 1 hr @ 850℃, 20 hrs @ 450℃ | | | | | | | |
|---|---|---|---|---|---|---|---|
| Specimen number | Thickness (mils) | Applied stress (MPa) | Cycles to failure Nf | Recoverable strain @ 1/2 Nf | Plastic strain @ 1/2 Nf | Recoverable strain @ Nf | Plastic strain @ Nf |
| 4 | 5 | 107 | 18338 | 0.0067 | 0.01406 | 0.00734 | 0.01926 |
| 5 | 5 | 103 | 58341 (run out) | 0.00495 | 0.01676 | 0.00425 | 0.01901 |
| 7 | 5 | 250 | 3035 | 0.01123 | 0.00956 | 0.01063 | 0.01669 |
| 6 | 10 | 226 | 8897 | 0.00955 | 0.01154 | 0.00895 | 0.02059 |
| 9 | 10 | 100 | 41463 | 0.00384 | 0.01581 | 0.00424 | 0.02473 |
| 10 | 10 | 250 | *creep like behavior - slip in grips* | | | | |
| 3 | 15 | 142 | *creep like behavior - slip in grips* | | | | |
| 1 | *Damaged during preliminary testing* | | | | | | |
| 2 | *Not applicable for isobaric uniaxial fatigue testing - irregular cross section with major notches* | | | | | | |
| 8 | *MTS tested* | | | | | | |

The following table is ordered according to increasing applied stress level.

| HT2 1 hr @ 850℃, 20 hrs @ 450℃ | | | | | | | |
|---|---|---|---|---|---|---|---|
| Specimen number | Thickness (mils) | Applied stress (MPa) | Cycles to failure Nf | Recoverable strain @ 1/2 Nf | Plastic strain @ 1/2 Nf | Recoverable strain @ Nf | Plastic strain @ Nf |
| 9 | 10 | 100 | 41463 | 0.00384 | 0.01581 | 0.00424 | 0.02473 |
| 5 | 5 | 103 | 58341 (run out) | 0.00495 | 0.01676 | 0.00425 | 0.01901 |
| 4 | 5 | 107 | 18338 | 0.0067 | 0.01406 | 0.00734 | 0.01926 |
| 3 | 15 | 142 | *creep like behavior - slip in grips* | | | | |
| 6 | 10 | 226 | 8897 | 0.00955 | 0.01154 | 0.00895 | 0.02059 |
| 7 | 5 | 250 | 3035 | 0.01123 | 0.00956 | 0.01063 | 0.01669 |
| 10 | 10 | 250 | *creep like behavior - slip in grips* | | | | |
| 1 | *Damaged during preliminary testing* | | | | | | |
| 2 | *Not applicable for isobaric uniaxial fatigue testing - irregular cross section with major notches* | | | | | | |
| 8 | *MTS tested* | | | | | | |

## 4. Heat Treatment Environment and Size Effect

### 4.1. Different processes

Two consecutive series of specimens were processed in two different manners. The first series was water-jet cut to the required dogbone dimensions and heat treated in high vacuum atmosphere while the second series was EDM cut and heat treated in air. The result is the observation of a major influence on the fatigue life of thin specimens while larger specimens don't seem to be so affected. Also, the existence of a consequential oxide layer is observed on the fracture surfaces of the failed specimens heat treated in air.

### 4.2. Influence on Stress – Life results

For the first series of specimens heat treated in high vacuum, the S-N curves didn't show much difference between the influence of the different thicknesses and of the two different heat treatments. However, the presence of an oxide layer led the thin specimens (0.005 in.) to fail prematurely while the thick ones sustained similar number of cycles to failure as the ones heat treated in high vacuum, as seen in the following result.

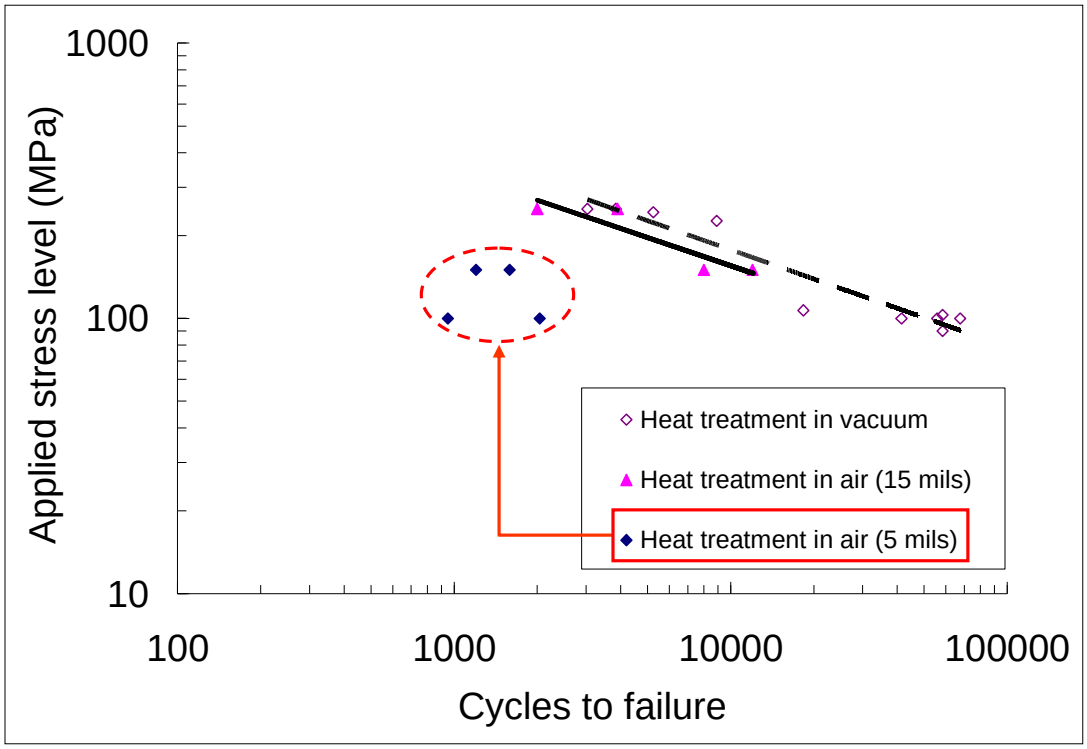

### 4.3. Assessment of microstructure through fractography

- Influence of thickness under identical stress level of 250MPa

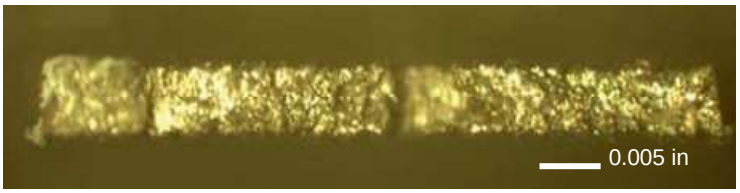


SP3 HT1 – thickness = 5 mils

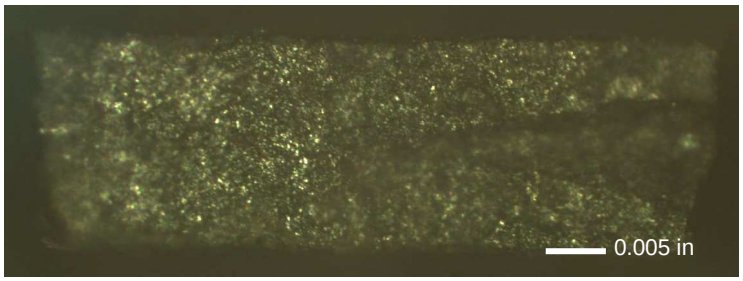


SP7 HT1 – thickness = 15 mils

Influence of thickness can be seen as cracks are generated across the thickness of SP3 HT1 where as SP7 HT1 displays more of a bulk behavior
Different failure behavior from thickness 5 mils to 15 mils

Transverse cracks and transverse tear up – strong dependency on the width to height ratio. Propagation of fatigue lines across the thickness.

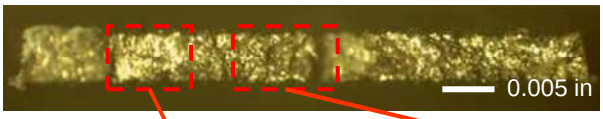


SP3 HT1 – thickness = 5 mils

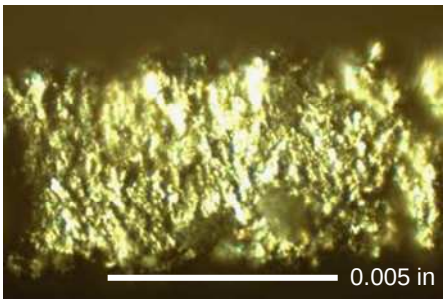


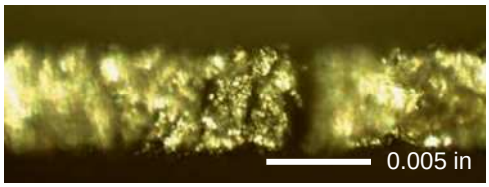


Thicker specimens display bulk behavior with random orientation of fatigue damage and propagation. Observation of a two stage failure: slow propagation and final tear up as in bulk material.

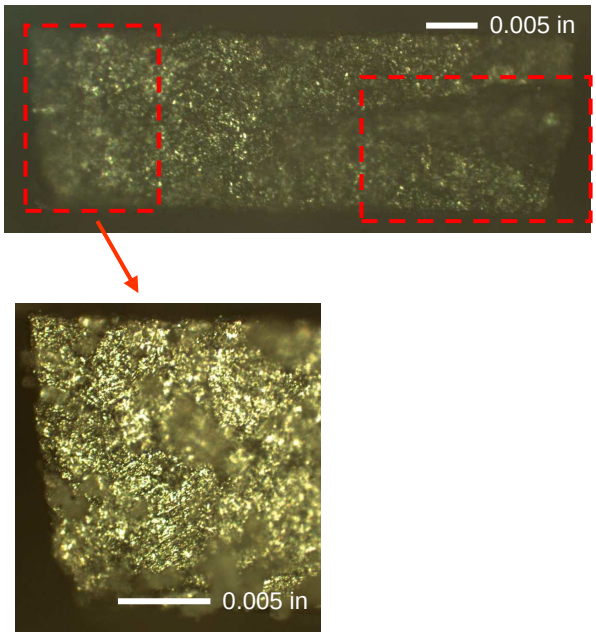


SP7 HT2 – thickness = 15 mils

The second series of specimens failed too early under 100MPa and 150MPa applied stress as a result of being heat treated in air instead of high vacuum atmosphere performed on the first series of specimens.

**HT in air, 100 -150 MPa**
**$N_f$ < 2000 cycles**


Fracture surface, thickness = 5 mils

**HT in vacuum, 100 – 150 MPa**
**$N_f \approx$ 50000 cycles**

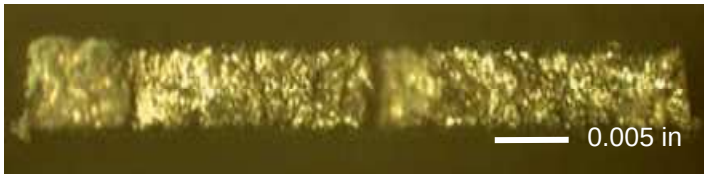


Fracture surface, thickness = 5 mils

Transverse fatigue lines across the thickness (as seen in vacuum heat treated specimens). Significant contrasted surface layer on the specimens: initial oxide layer formed upon heat treatment. Interface is clear and cracks can be identified.

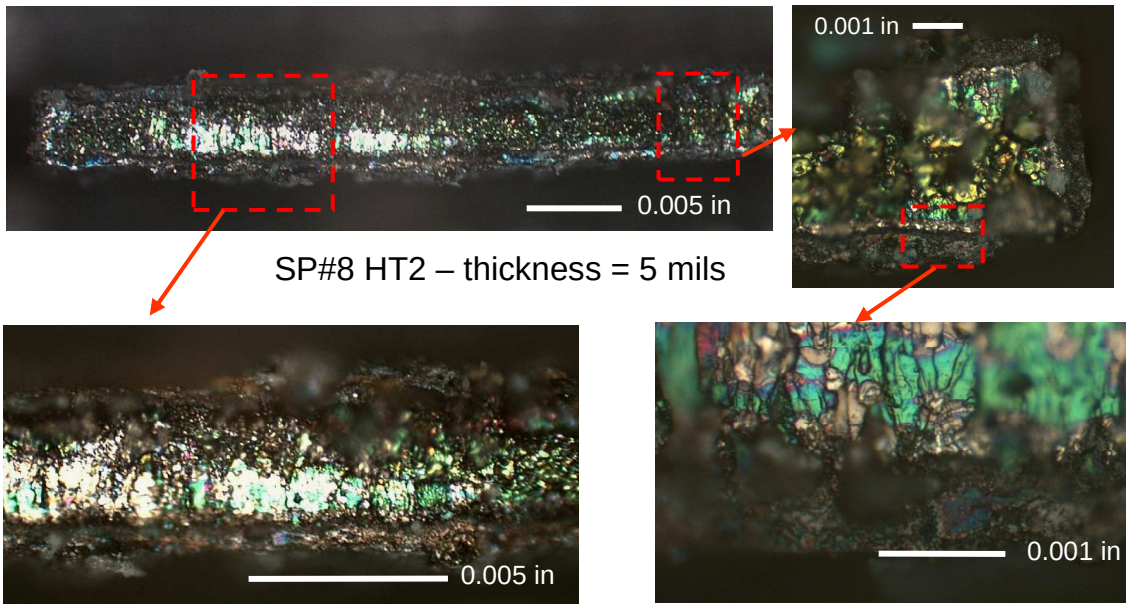


Thick specimens exhibit oxide layer of similar thickness
Oxide layer is less influential on thicker specimens (smaller proportion of oxide layer in thick specimens). Shear stresses at SMA/oxide interface

⇒ Crack initiation with partial loss of random fatigue lines distribution.

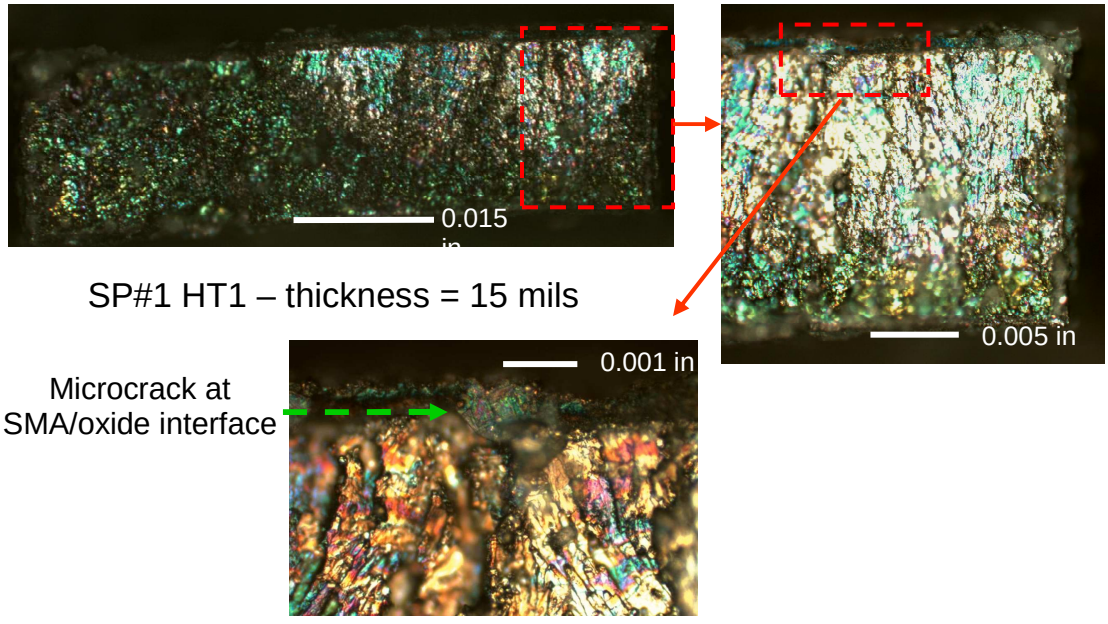

Preliminary secondary electron microscopy (SEM) observations of fatigue striations: initiation, propagation and final failure. The thin specimen shows initiation at one edge with propagation across the width until the cracks became unstable and the specimen failed.

The cracks that formed during propagation and before final failure seem to all be oriented transversely to the thickness.

The thicker specimens however display two main initiation zones, and then propagation appears to take place mostly across the thickness.
In the thicker specimens, the cracks appear more serrated, with an intergranular aspect while the thin specimens seemed more to have undergone transgranular cracks.

- **Fracture surfaces for Vacuum HT#1**

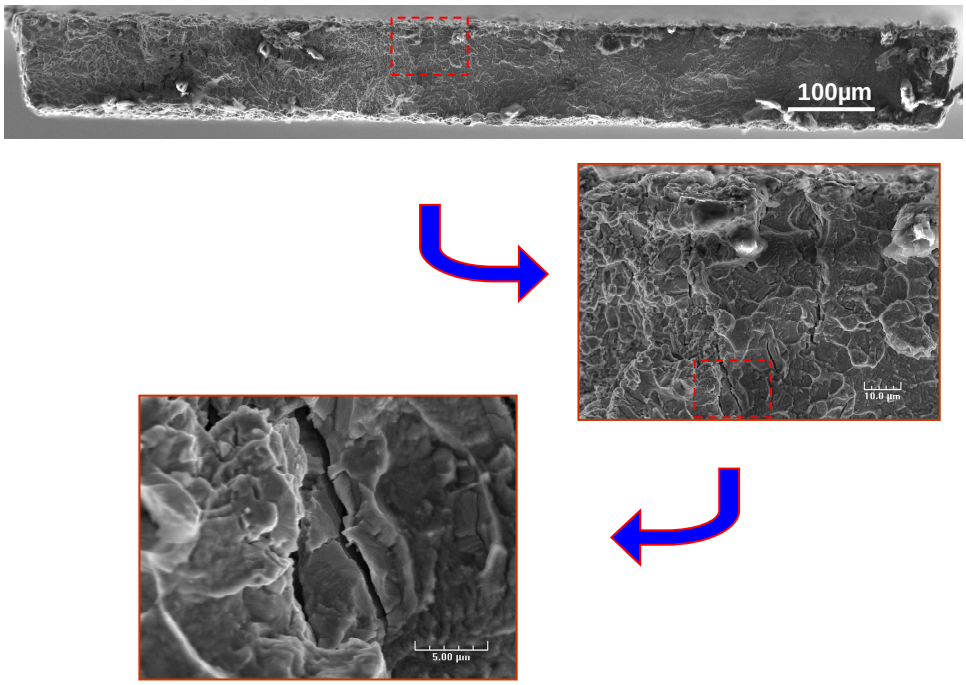


SP#10 HT1 - 5 mils – 100MPa

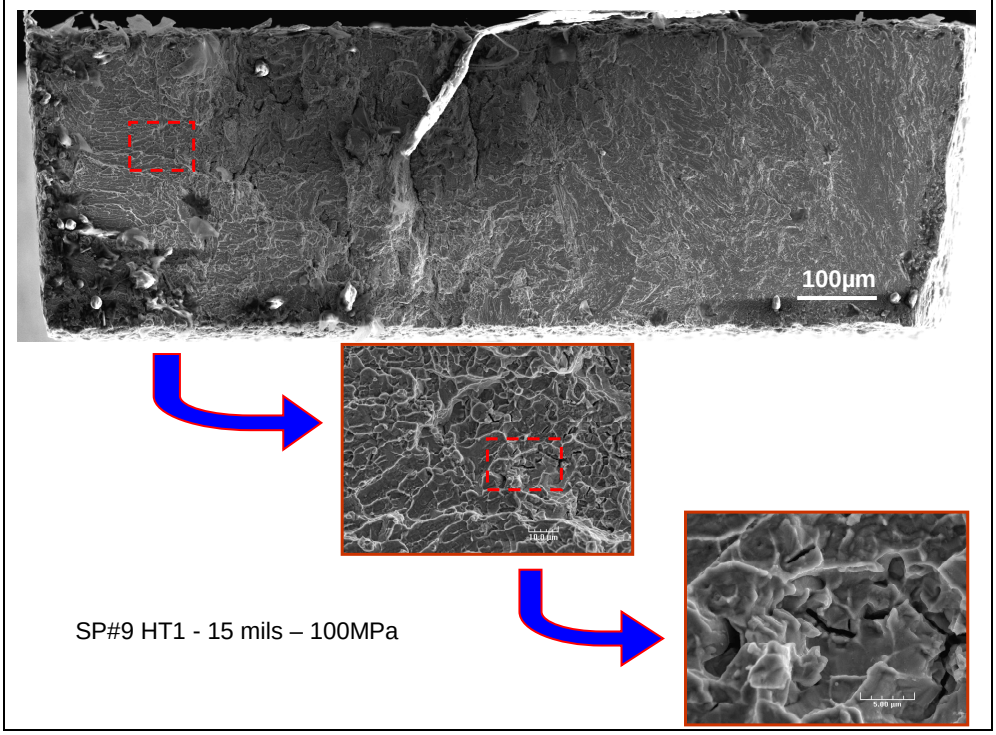


SP#9 HT1 - 15 mils – 100MPa

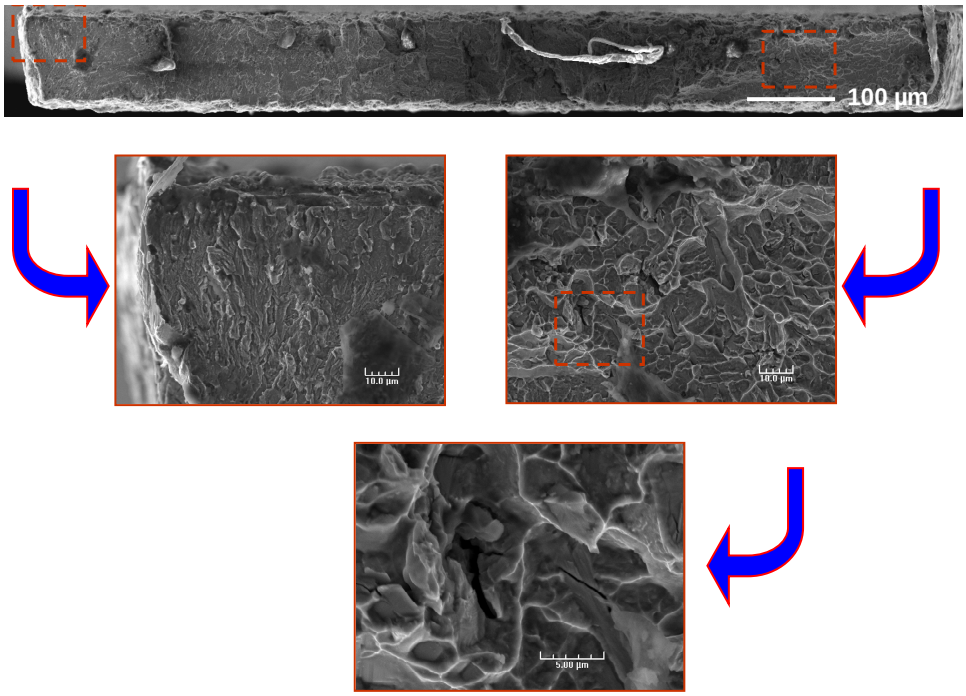


SP#3 HT1 - 5 mils – 250MPa

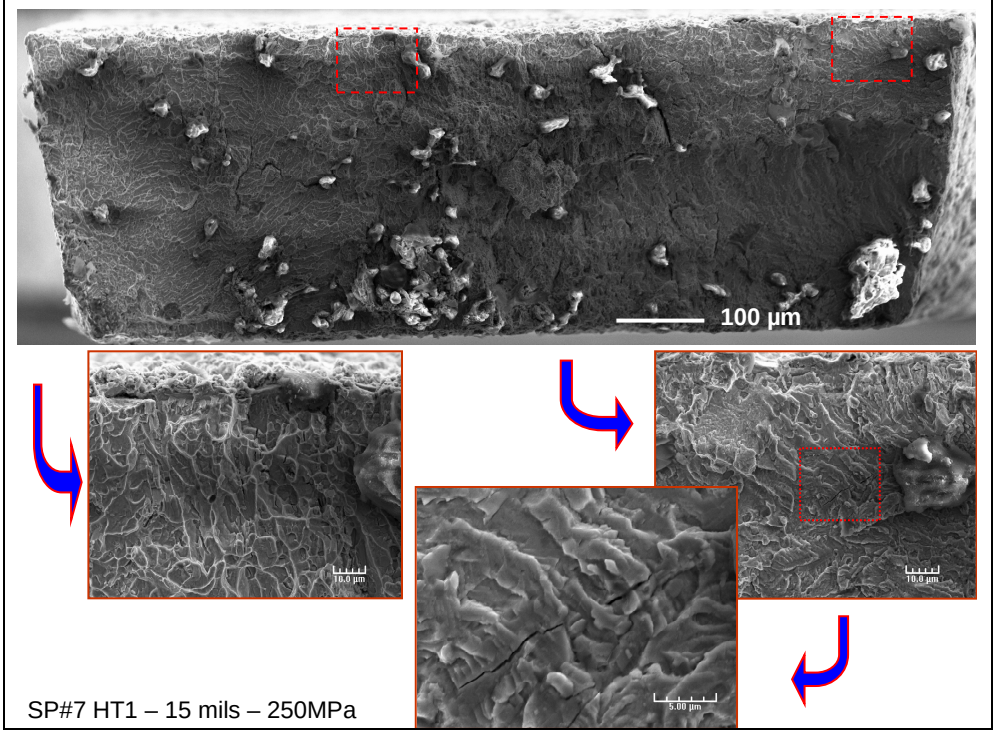


SP#7 HT1 – 15 mils – 250MPa

- **Fracture surfaces for Vacuum HT#2**

The following micrographs represent fracture surfaces for vacuum HT#2, in the case of 100MPa and 250MPa applied load, respectively. Much different fracture surfaces in this case from the HT#1. A more ordered structure, with larger propagation zones and clear evidence of a high precipitate / inclusion content.

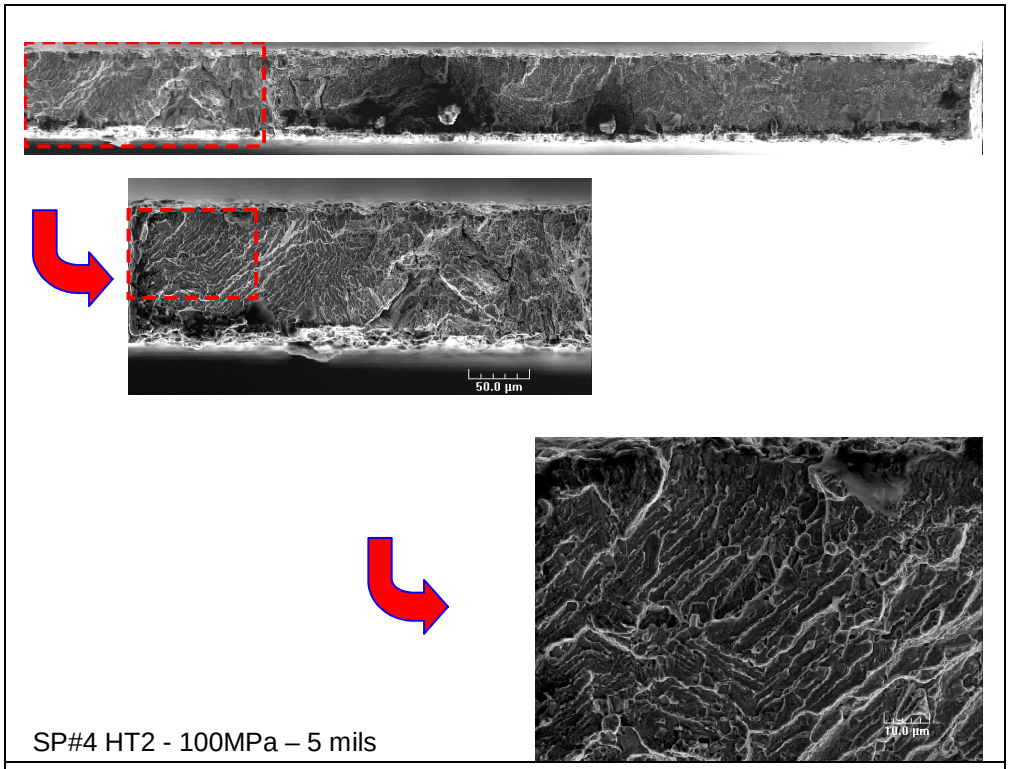


SP#4 HT2 - 100MPa – 5 mils

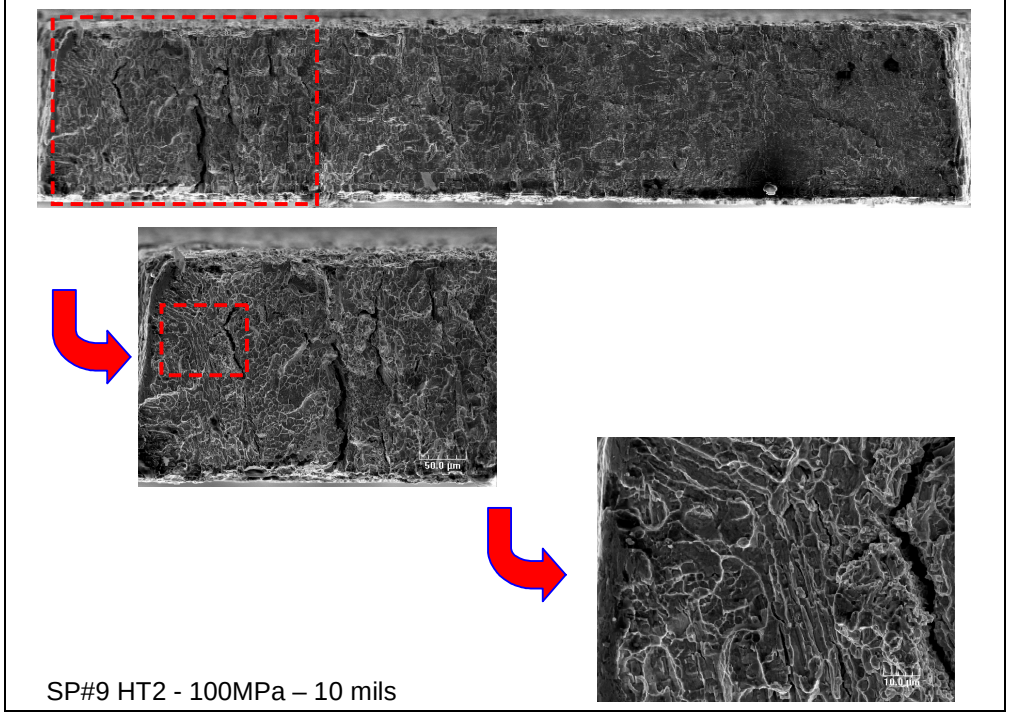


SP#9 HT2 - 100MPa – 10 mils

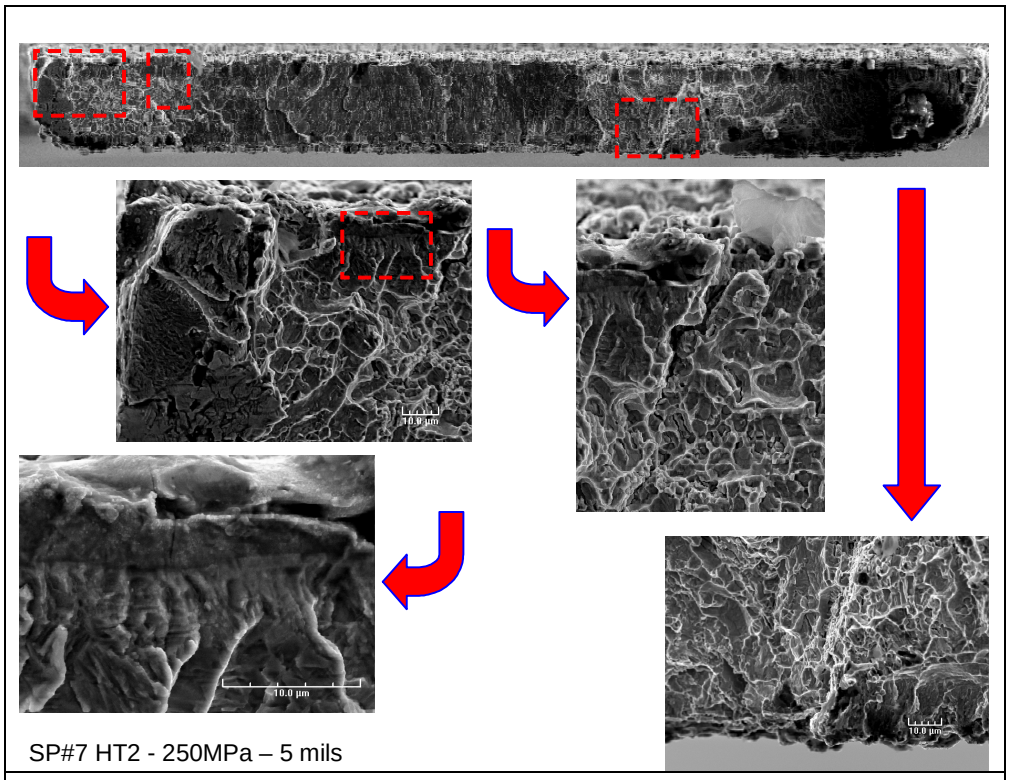

SP#7 HT2 - 250MPa – 5 mils

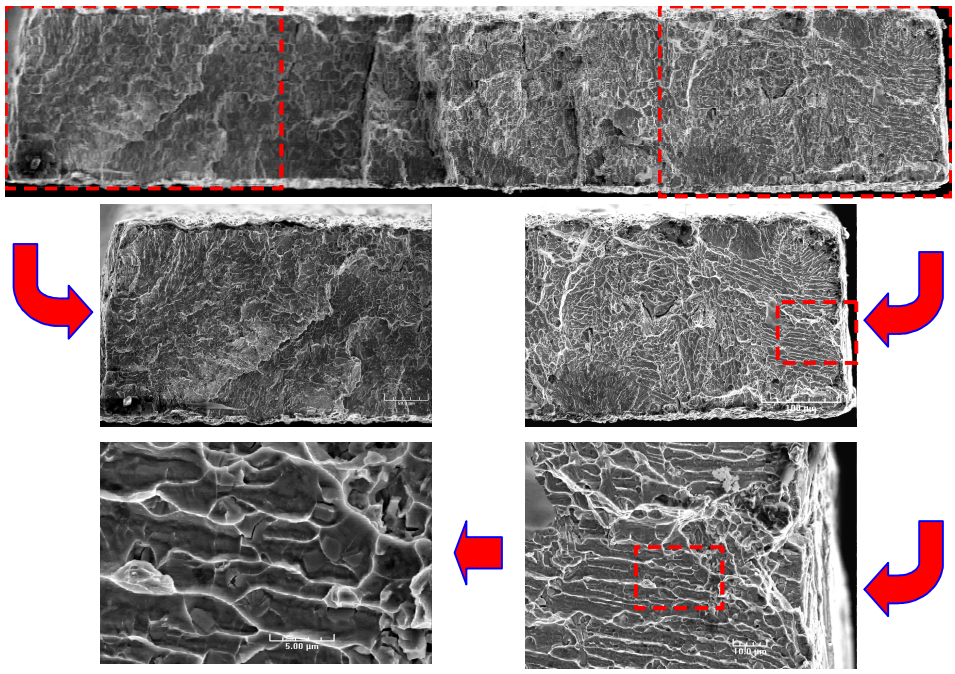

SP#10 HT2 - 250MPa – 10 mils

### 4.4 Comparison between 60-NiTi and 57-NiTi fatigue behaviors

A different composition of NiTi with expected similar properties is being investigated to assess any difference or similarities. The selected composition is 57Ni43Ti (wt.%, referred to as 57-NiTi). The heat treatment that was applied corresponds to the heat treatment #2 in air. Two tests were achieved under 100MPa and two others under 250MPa. The corresponding strain – life curves are reported in the following plots.

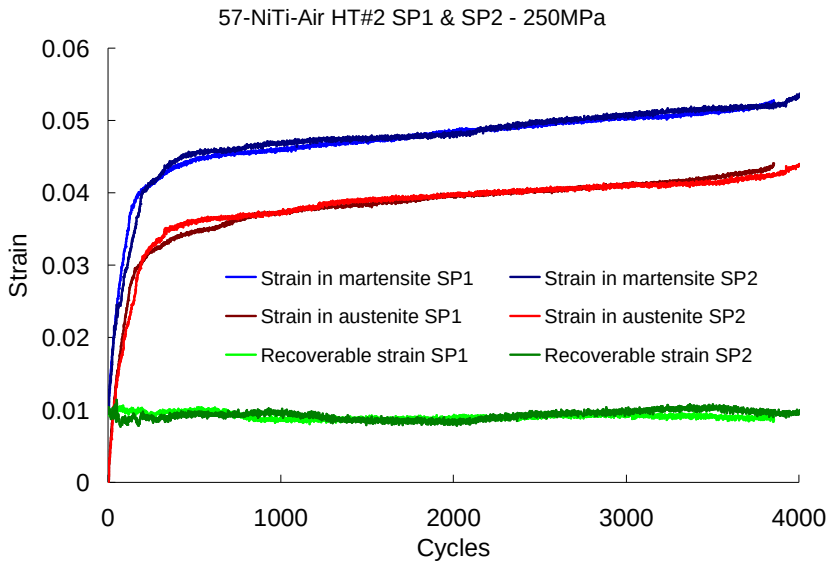


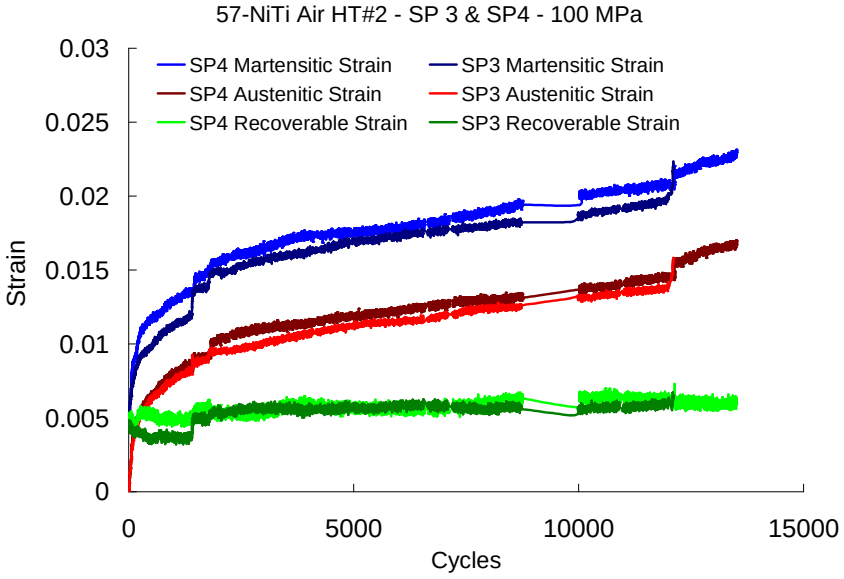


In the following stress – life results, under high applied stress (250MPa), 57-NiTi shows good properties with consistent results with 60-NiTi. However, under 100MPa, the life of

the 57-NiTi actuators is much less than the 60-NiTi one. Results for 60-NiTi air HT at 15 mils and results for 57-NiTi air HT at 15 mils as well allow us to compare only composition variation influence. The slightly higher fatigue life of 57-NiTi under 250MPa can be explained by the fact that on the previous strain – life plots, the plastic strain is rapidly stabilized and exhibits a better stabilized regime than the one seen in 60-NiTi fatigue cyclic behavior. At lower applied stress levels, 57-NiTi shows poor fatigue properties and fails earlier than the 60-NiTi.

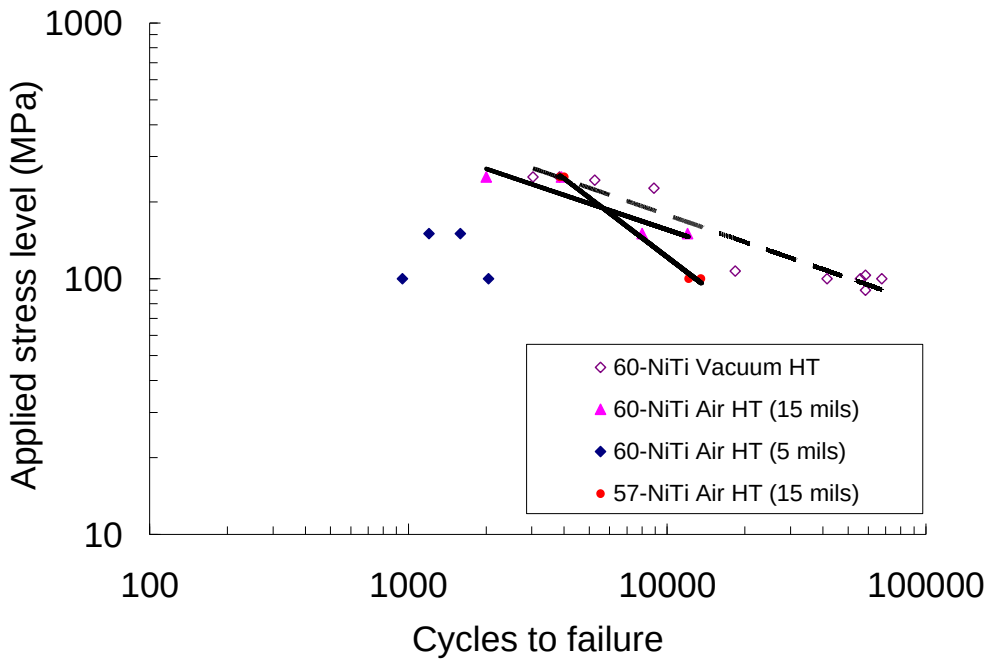


This behavior can be confirmed in the plastic strain – cycles to failure plot seen below. Results for 57-NiTi yield a much narrower cycles to failure range compared to the one in 60-NiTi for a similar applied stress range. Plastic strain in this case appears to have a very strong influence on the response of the SMA.

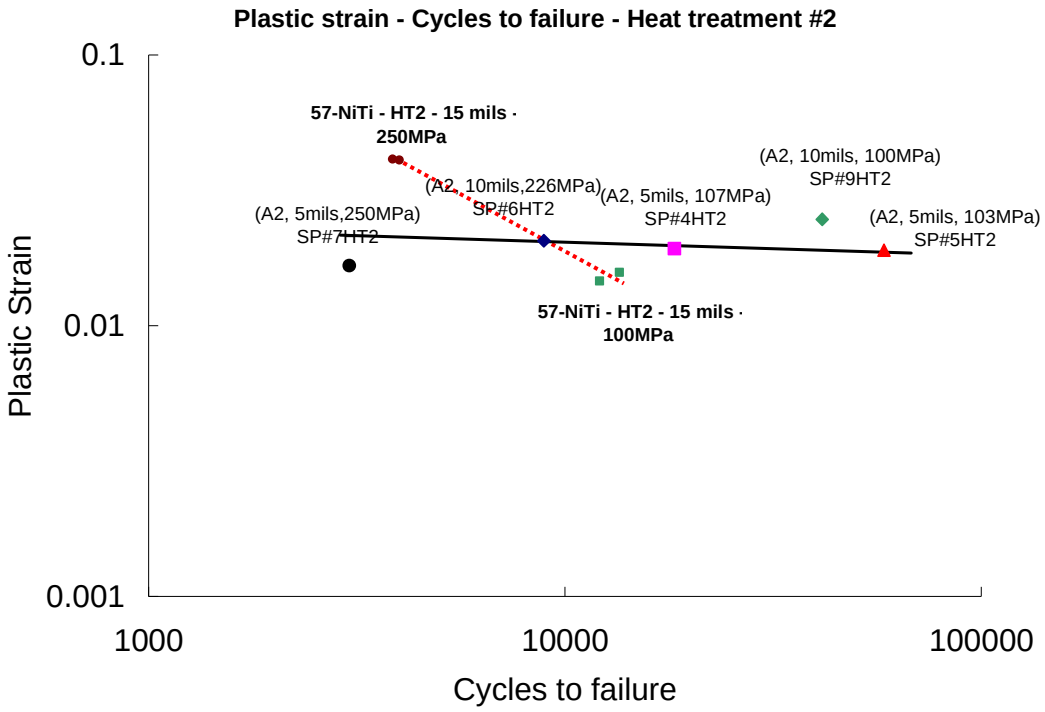
Plastic strain - Cycles to failure - Heat treatment #2
0.1
0.01
0.001
Plastic Strain
1000
10000
100000
Cycles to failure
57-NiTi - HT2 - 15 mils - 250MPa
(A2, 10mils,226MPa) SP#6HT2
(A2, 5mils, 107MPa) SP#4HT2
(A2, 10mils, 100MPa) SP#9HT2
(A2, 5mils,250MPa) SP#7HT2
(A2, 5mils, 103MPa) SP#5HT2
57-NiTi - HT2 - 15 mils - 100MPa